GDP and GTP Association Equilibria. Use of Manganous Ion Induced Paramagnetic Relaxation Rates To Study Hydrogen-Bonded Species

G. Edwin Wilson,*,†,‡ Christopher J. Falzone,†,‡ and Hao Dong†

Contribution from the Department of Chemistry, The University of Akron, Akron, Ohio 44325, and Department of Chemistry, Clarkson University, Potsdam, New York 13676.
Received December 18, 1989

Abstract: The nucleotide concentration dependence of H-8 chemical shifts and the manganous ion induced paramagnetic relaxation rates of GDP and GTP have been studied at pH 8.2 and 25 °C by ^1H, ^{13}C, and ^{31}P NMR spectroscopy. The paramagnetic relaxation rate of H-8 increased with the nucleotide concentration from 0 to 100 mM, plateaued from 100 to 190 mM nucleotide, and then decreased for a change of nucleotide concentration from 190 to 250 mM. This behavior is consistent with an initial association of monomers to form stacked dimers followed by association of the stacked species through hydrogen bonding to form a species proposed to be an octamer. The phosphate groups and N-7 are the primary and secondary binding sites of the manganous ion in the dimer. Average Mn–C distances of the complexed dimers are consistent with a head-to-tail stacked arrangement in which N-9 of both nucleotides lies on the same edge of the stack. The data are consistent with the interpretation that the hydrogen-bonded octamers are stacked tetramers of guanosines arranged circularly with N-7 and the carbonyl oxygen hydrogen bonded to the amino nitrogen and N-1, respectively. Because N-7 is involved in the hydrogen bonding of the octamer, it is unavailable for association with manganous ions.

Studies of the structure of nucleotides in solution, particularly by NMR techniques, have been an intense area of investigation.[1,2] Adenosine nucleotides have received the most attention, largely because of their major role in metabolic processes. Except for guanosine monophosphate,[3-9] the guanosine nucleotides have been largely neglected. Because of the importance of guanosine di- and triphosphates in a number of biological processes, we have undertaken a study of their solution structures using NMR techniques with the manganous ion as a paramagnetic probe.

Rapidly exchanging paramagnetic metal ions are routinely used to probe the structures of ligands by means of NMR spectroscopy. When more than one equilibrium between bound and free ligand exists and the complexes have different average distances between the metal and the ligand nuclei, the concentration dependence of paramagnetic relaxation rates should be a sensitive probe of the various equilibria. Here we describe what we believe to be the first application of this concept to elucidate competing stacking and octamer-forming equilibria of guanosine di- and triphosphates.

Experimental Section

The sodium salts of GDP and GTP were purchased from Sigma Chemical Co. Paramagnetic impurities were removed by passing nucleotide solutions at pH 7 through a Chelex-100 column (1 × 25 cm) previously washed with water and equilibrated at pH 7. The nucleotide solution was adjusted to pH 8.2 with sodium hydroxide and lyophilized. For the ^1H NMR studies, paramagnetic metal ion free nucleotide solutions were lyophilized three times from D_2O. Nucleotide concentrations were determined spectrophotometrically at 252 nm (ϵ = 13 700, pH 7). The Mn^{2+} was added by disposable microliter pipet from solutions prepared from standardized stock solutions of $MnCl_2 \cdot 6(H_2O)$ (J. T. Baker).

All nucleotide spectra were collected at 25 °C in 99.9% D_2O solutions by using multinuclear JEOL FX-90Q, Varian FT-80, or Varian VXR-300 spectrometers equipped with variable-temperature accessories. Chemical shifts for H-8 of GDP were measured by using *tert*-butyl alcohol as an internal chemical shift standard. The nucleotide solutions contained 2 mM EDTA to complex paramagnetic impurities. Free induction decays of 8K data points were stored and Fourier transformed to produce spectra with digital resolutions of 0.24 Hz for ^1H (89.56 MHz), 0.49 Hz for ^{31}P (36.28 MHz), and 0.61 Hz for ^{13}C (22.53 MHz). Carbon and phosphorus spin–lattice relaxation times were determined by using a saturation–recovery pulse sequence. At least 700 transients were collected for ^{13}C data, and at least 20 scans were obtained for the ^{31}P spectra. Proton spin–lattice relaxation times were determined by use of an inversion–recovery pulse sequence. The T_1 data were analyzed by a nonlinear least-squares procedure. The molar paramagnetic spin–lattice relaxation rates were calculated from slopes of plots of paramagnetic relaxation rates as a function of the metal to nucleotide ratio.

Paramagnetic Relaxation. For nucleotide systems complexing with manganous ions, the molar paramagnetic longitudinal relaxation rate is given by

$$T_{1M}^{-1} = \frac{C}{r^6}\left(\frac{3\tau_c}{1+\omega_I^2\tau_c^2} + \frac{7\tau_c}{1+\omega_S^2\tau_c^2}\right) \quad (1)$$

where C is a collection of constant terms, ω_I and ω_S are the nuclear and electron Larmor frequencies, and τ_c is the correlation time for dipolar interactions given by

$$\tau_c^{-1} = \tau_r^{-1} + \tau_s^{-1} + \tau_M^{-1} \quad (2)$$

where τ_r is the rotational correlation time, τ_s is the electron spin relaxation time, and τ_M is the mean time a nucleus spends in the coordination sphere of the paramagnetic ion.[10,11]

The shortest relevant correlation time dominates τ_c, and for small molecules, this is generally τ_r. The value of τ_r has been determined to be on the order of (1–3) × 10^{-10} s for adenine nucleotides.[12,13] In this study, τ_r was determined to be 3 × 10^{-10} s, based on the frequency dependences of the paramagnetic relaxation times of H-8 and H-1′ of GDP at three concentrations. The value of τ_s for the manganous ion[14] is ca. 10^{-8} s. The value of τ_M for water exchange at manganous ion[15] is

* Address correspondence to this author at The University of Akron.
† The University of Akron.
‡ Clarkson University.

(1) Pezzano, H.; Podo, F. *Chem. Rev.* **1980**, *80*, 365–401.
(2) Marzilli, L. G. *Prog. Inorg. Chem.* **1977**, *23*, 255–378.
(3) Pinnavaia, T. J.; Marshall, C. L.; Mettler, C. M.; Fisk, C. L.; Miles, H. T.; Becker, E. D. *J. Am. Chem. Soc.* **1978**, *100*, 3625–3627.
(4) Pinnavaia, T. J.; Miles, H. T.; Becker, E. D. *J. Am. Chem. Soc.* **1975**, *97*, 7198–7200.
(5) Borzo, M.; Detellier, C.; Laszlo, P.; Paris, A. *J. Am. Chem. Soc.* **1980**, *102*, 1124–1134.
(6) Detellier, C.; Laszlo, P. *J. Am. Chem. Soc.* **1980**, *102*, 1135–1141.
(7) Walmsley, J. A.; Barr, R. G.; Bouhoutsos-Brown, E.; Pinnavaia, T. J. *J. Phys. Chem.* **1984**, *88*, 2599–2605.
(8) Bouhoutsos-Brown, E.; Marshall, C. L.; Pinnavaia, T. J. *J. Am. Chem. Soc.* **1982**, *104*, 6576–6584.
(9) Led, J. J.; Gesmar, H. *J. Phys. Chem.* **1985**, *89*, 583–588.
(10) Solomon, I. *Phys. Rev.* **1955**, *99*, 559–565.
(11) Bloembergen, N. *J. Chem. Phys.* **1957**, *27*, 572–573.
(12) Lam, Y.-F.; Kuntz, G. P. P.; Kotowycz, G. *J. Am. Chem. Soc.* **1974**, *96*, 1834–1839.
(13) Sternlicht, H.; Shulman, R. G.; Anderson, E. W. *J. Chem. Phys.* **1965**, *43*, 3123–3132.
(14) Kotowycz, G.; Hayamizu, K. *Biochemistry* **1973**, *12*, 517–520.
(15) Swift, T. J.; Connick, R. E. *J. Chem. Phys.* **1962**, *37*, 307–320.

0002-7863/90/1512-8269$02.50/0

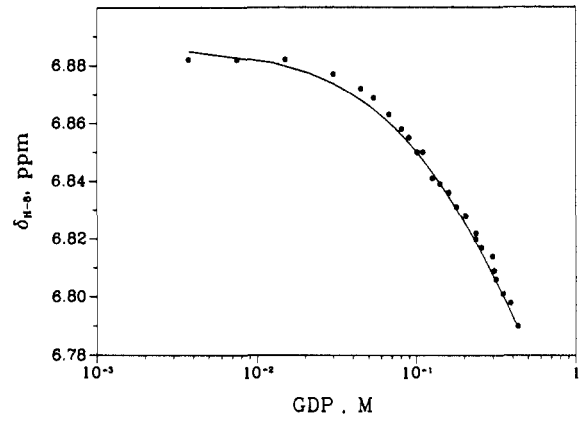

Figure 1. Dependence of H-8 chemical shift on GDP concentration at pH 8.2. The solid line is the calculated curve by using eq 5.

6.3×10^{-8} s, and τ_M for exchange of the phosphates of ATP out of the coordination sphere of manganese in Mn(II)–ATP[16] is 6.5×10^{-6} s. Thus, τ_r seems to be dominant in eq 1 for metal interactions with either the nucleotide ring or the phosphate groups.

In the presence of ligand exchange between the bulk solution and the metal coordination sphere, the paramagnetic contribution to the relaxation rate, T_{1p}^{-1} is given by[15,17]

$$T_{1p}^{-1} = T_{1_{obs}}^{-1} - T_{1_0}^{-1} = \frac{np}{(T_{1M} + \tau_M)} + T_{1_\infty}^{-1} \quad (3)$$

where T_{1obs}^{-1} is the observed relaxation rate in the presence of paramagnetic ion, T_{10}^{-1} is the relaxation rate in the absence of paramagnetic ion, p is the concentration ratio of paramagnetic ion to the total ligand, n is the number of coordinated ligands per paramagnetic ion, and $T_{1_\infty}^{-1}$ is the dipolar contribution to the average relaxation rate of the nucleus by molecules outside the first coordination sphere of the paramagnetic ions.

Results

Concentration Dependence of Chemical Shifts. The upfield movement of nucleotide base chemical shifts accompanying an increase in their concentration is associated with base stacking. In the isodesmic model for this effect, nucleotide stacking is considered to be a noncooperative association of an indefinite number of monomers with an equilibrium constant given by[18,19]

$$K = [N_{n+1}]/[N_n][N] \quad (4)$$

where N_n represents a stack of nucleotides n units long, and where equality of all equilibrium constants for monomer addition to the stack is assumed. The variation of chemical shift as a function of the equilibrium constant K and the total nucleotide concentration $[N]_0$ is then given by[20]

$$\omega_{obs} = \omega + (\omega - \omega_0)\left(1 - \frac{(4K[N]_0 + 1)^{1/2}}{2K[N]_0}\right) \quad (5)$$

where ω_0 is the chemical shift at infinite dilution and ω is the shift of an infinitely long nucleotide stack.

The concentration dependence of the GDP H-8 chemical shift shown in Figure 1 was used to calculate an isodesmic dissociation constant of 1.43 M^{-1} for GDP by using the infinitely long stack assumption. This dissociation constant compares favorably with the value of 1.29 M^{-1} for 5′-GMP obtained by Neurohr and Mantsch.[21] At 90 MHz the total upfield shift range for GDP concentrations from 4 to 440 mM was 8.3 Hz. Assuming the infinite stack model and that no other association mechanisms exist, the model predicts dimers exist to the extent of ~20% at a GDP concentration of 100 mM.

Concentration Dependence of Relaxation Rates. The relaxation rates of H-1′ and H-8 of GDP (Table I) were measured at 300

Table I. Proton Molar Relaxation Rates of Guanosine Diphosphate at 80 and 300 MHz

	T_1, s			
	80 MHz		300 MHz	
concn, M	H-8	H-1′	H-8	H-1′
0.036	0.95	1.79	1.42	2.23
0.16	0.50	1.05	0.64	1.31
0.23	0.58	0.84	1.20	1.50

Table II. Calculated Distances from the Manganous Ion to ^1H, ^{13}C, and ^{31}P Nuclei of Guanosine Nucleotides at Various Concentrations and the Respective Molar Paramagnetic Spin–Lattice Relaxation Rates

nucleotide	atom	r, Å	$1/T_{1M}$, $s^{-1} \times 10^2$	[nucleotide], mM
GDP	C-2	5.1	9.77	190
	C-4	5.2	8.02	190
	C-5	4.1	34.7	190
	C-6	3.8	52.6	190
	C-8	3.5	90.2	190
	P-α	3.0	557.2	153
	P-β	3.2	433.2	153
	H-8	5.4	103.7	34
	H-8	4.2	448.9	50
	H-8	4.0	611.0	75
	H-8	4.0	607.3	122
	H-8	4.1	540.8	178
	H-8	4.0	616.7	190
	H-8	5.5	87.6	262
	H-1′	7.7	12.2	34
	H-1′	5.7	73.1	122
	H-1′	5.9	62.0	190
GTP	C-2	5.3	7.2	222
	C-4	5.5	5.8	222
	C-5	4.5	21.0	222
	C-6	4.6	16.9	222
	C-8	4.2	28.0	230
	P-α	3.3	319.0	265
	P-β	3.2	426.3	265
	P-γ	3.2	406.5	265
	H-8	5.9	58.2	8
	H-8	5.2	123.6	18
	H-8	4.0	657.9	124
	H-8	4.6	265.9	222
	H-1′	7.1	19.4	8
	H-1′	5.8	66.4	124

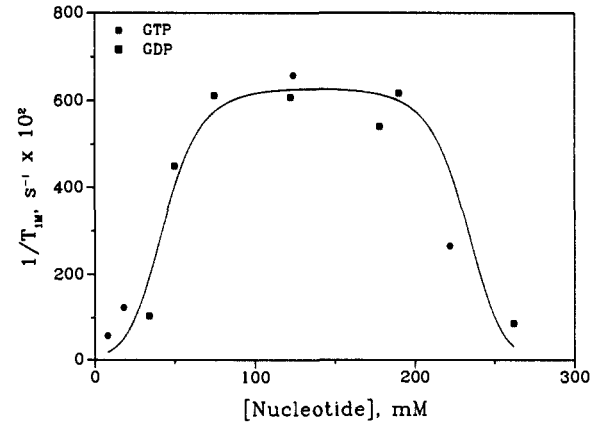

Figure 2. Dependence of molar spin–lattice paramagnetic relaxation rate of H-8 of GDP (■) and GTP (●) on nucleotide concentration at pH 8.2.

(16) Brown, F. F.; Campbell, I. D.; Henson, R.; Hirst, C. W. J.; Richards, R. E. *Eur. J. Biochem.* **1973**, *38*, 54–58.
(17) Luz, Z.; Meiboom, S. *J. Chem. Phys.* **1964**, *40*, 2686–2692.
(18) Heyn, M. P.; Bretz, R. *Biophys. Chem.* **1975**, *3*, 35–45.
(19) Heyn, M. P.; Nicola, C. U.; Schwartz, G. *J. Phys. Chem.* **1977**, *81*, 1611–1617.
(20) Mitchell, P. R.; Sigel, H. *Eur. J. Biochem.* **1978**, *88*, 149–154.
(21) Neurohr, K. J.; Mantsch, H. H. *Can. J. Chem.* **1979**, *57*, 1986–1994.

and 80 MHz for nucleotide concentrations of 0.036, 0.16, and 0.23 M, and these were used to calculate τ_c. The frequency depenence of the relaxation rate ratios led to τ_c values of 1.6×10^{-10}, 1.5×10^{-10}, and 2.8×10^{-10} s for H-1′. The corresponding correlation times for H-8 were 2.2×10^{-10}, 1.6×10^{-10}, and 3.4×10^{-10} s.

The average molar paramagnetic relaxation rates for H-8 of GDP and GTP were found to be functions of concentration of the nucleotide (Table II, Figure 2). The concentration dependence of the H-8 molar paramagnetic relaxation rates of both GDP and GTP were nearly identical over the concentration range of 34–75 mM, roughly paralleling the 2-fold increase in the concentrations of dimer and higher complexes calculated from the concentration dependence of the H-8 chemical shift. In the range 80–190 mM, little change was observed in the molar paramagnetic relaxation rates of H-8; however, a 2-fold increase in total concentrations of dimers and higher stacked complexes of GDP is expected based on the isodesmic dissociation constant. Thus, the plateau region appears to represent a balance between at least two competing equilibria, the first characterized by a strong manganous ion dipolar interaction with H-8 and the second characterized by a decrease in this interaction. For reasons described below, we believe the second equilibrium to be associated with the formation of an octamer from stacked dimers. At nucleotide concentrations above 190 mM, the molar paramagnetic rate is observed to decrease. Comparison of Figures 1 and 2 indicates that the concentration dependences of the proton chemical shift and paramagnetic relaxation rate probe different equilibria. The H-8 chemical shift is not a sensitive probe for the second equilibrium, but the paramagnetic relaxation rate is sensitive to both stacking and the second equilibrium.

If the molar paramagnetic relaxation rate of H-8 is probing a pure stacking equilibrium, it should increase as the average stack size grows from monomer to dimer to oligomer, eventually arriving at a plateau value. This saturation behavior should occur because the relaxation rate depends on the number of nucleotide H-8 protons close to the manganous ion. Since the number of nearby H-8 protons is two for manganous ion binding to a terminal nucleotide or three for binding to a nonterminal nucleotide, a rate plateau should be achieved as the stack length increases. Since saturation behavior is predicted by this model, the observed behavior must have an origin with a process other than stacking.

Changes in either the correlation time or the outer-sphere relaxation rate with increased nucleotide concentration could cause the concentration-dependent decrease in the paramagnetic relaxation rate at high nucleotide concentrations according to eqs 1 and 3. However, the nucleotide correlation times change by a factor of ~2 over the same concentration range for which the paramagnetic relaxation rate decreases by nearly an order of magnitude. Outer-sphere relaxation cannot be a major contributor to the paramagnetic relaxation rate since this would cause the paramagnetic relaxation rate to increase with increasing nucleotide concentration, and this is counter to the observed trend.

Structures of Nucleotide Dimers. Manganous ion paramagnetic contributions to the molar ^{31}P spin–lattice relaxation rates for the phosphorus atoms in GDP and GTP are similar (Table II). The larger paramagnetic spin–lattice relaxation rate of P-α of GDP indicates a slightly shorter distance from the manganous ion to P-β (3.1 Å) than that for P-α (3.2 Å). The β- and γ-phosphorus atoms of GTP show slightly shorter distances than that for the α-phosphorus atom; however, the calculated P–Mn distances for both GDP and GTP complexes indicate that the phosphate chain is directly bound to the manganous ion. In addition, the calculated distances are in good agreement with the X-ray distance found for the $LiMnPO_4$ crystal (3.3 Å).[22]

The paramagnetic contributions of the manganous ion to the ^{13}C spin–lattice relaxation rates for C-2, C-4, C-5, C-6, and C-8 as functions of the paramagnetic ion to total nucleotide ratios in a 190 mM GDP solution at pH 8.2, where the predominant species is the stacked dimer, are shown in Figure 3. The paramagnetic contribution to the ^{13}C spin–lattice relaxation rate of 222 mM

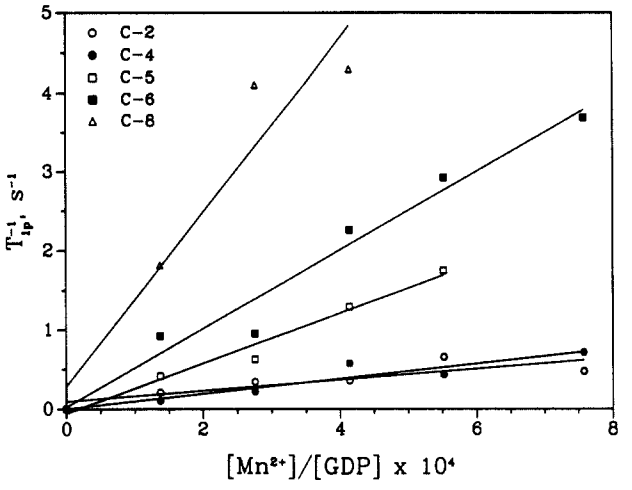

Figure 3. Dependence of molar paramagnetic spin–lattice relaxation rates of C-2, C-4, C-5, C-6, and C-8 on manganous ion concentration in 190 mM GDP at pH 8.2.

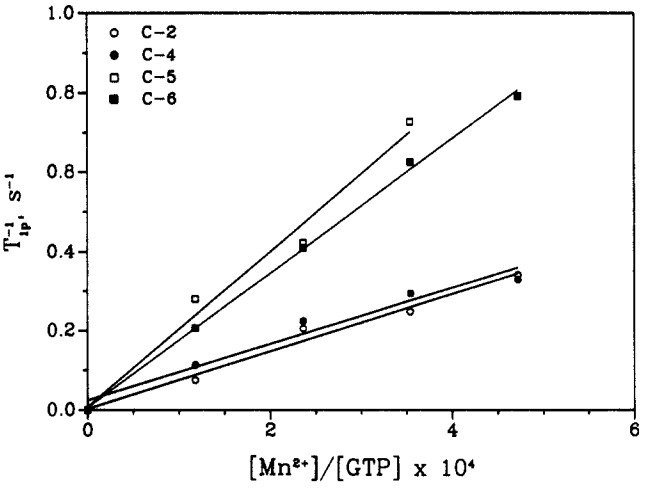

Figure 4. Dependence of molar paramagnetic spin–lattice relaxation rates of C-2, C-4, C-5, and C-6 on manganous ion concentration in 222 mM GTP at pH 8.2.

GTP at pH 8.2 as a function of the ratio [Mn]/[GTP] is shown in Figure 4 for C-2, C-4, C-5, and C-6. The T_{1M}^{-1} value for C-8 was determined in a separate experiment on a solution that was 230 mM in GTP. The molar relaxation rates are given in Table II. The distances calculated from the slopes in Figures 3 and 4 fall naturally into two categories, C-5, C-6, and C-8 being closer to and relaxed faster by the manganous ion than are C-2 and C-4. This suggests that the metal in the stacked dimer is close to N-7 of the purine ring and remote from C-2. The similarity of the distances from C-2 and C-4 to the manganous ion in the dimer is not expected in the 1:1 metal ion–nucleotide complex and implies that the stacking arrangement is characterized by a shorter distance from the metal ion to C-2.

Discussion

The combination of chemical shift and paramagnetic relaxation data allows a rather complete description of the structures of complexes present in solutions of GDP and GTP. At concentrations in the range 10–190 mM, the dominant species in solution ranges from monomeric nucleotide at the lower concentrations to stacked dimers at the higher concentrations. The formation of dimers is characterized by a decrease in the apparent average manganous ion–H-8 distance by ~1.9 Å from its monomeric value of 5.9 Å and by a decrease in the H-8 chemical shift. An equilibrium constant of 1.43 M^{-1} can be calculated from the concentration dependence of the chemical shift. At concentrations above ~190 mM a third species, which is consistent with an

(22) Geller, S.; Durand, J. L. *Acta Crystallogr.* **1960**, *13*, 325–331.

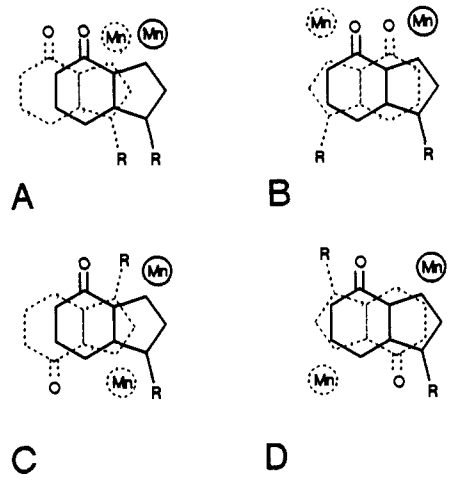

Figure 5. Orientations of guanosine units in stacked nucleotides.

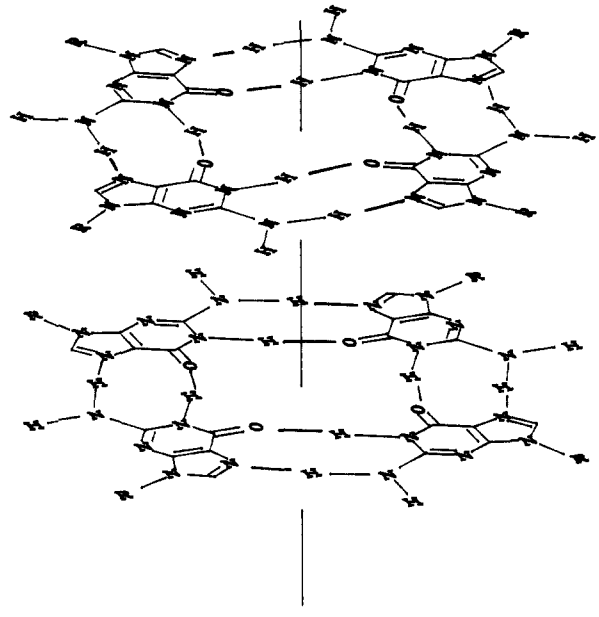

Figure 6. Stacked octamer of guanosine nucleotides.

octamer (vide infra), contributes to the solution structure of GDP and GTP. The increase in octamer concentration is characterized by an increase in the average distance from the manganous ion probe to the nucleotide H-8 with increasing nucleotide concentration.

The structure of the stacked dimers may be inferred from paramagnetic relaxation rate data on the nucleotide carbon atoms. The distances between the manganous ion and purine ring carbons at a concentration of 220 mM, where stacked dimers predominate, is incompatible with those expected for any conformation with a single set of manganese–carbon distances. Because of the short contacts to C-6, C-5, and C-8, the manganous ion must be located near N-7 of at least one guanosine ring, consistent with findings for manganous complexes of adenine nucleotides[12,13,23] and the crystal structures of $Mn(GMP)(H_2O)_5$ and $Ni(GMP)(H_2O)_5$.[24,25] The distances from the manganous ion to C-6, C-5, and C-8 (3.8, 4.1, and 3.5 Å) are close to those expected (ca. 3.6, 3.3, and 3.3 Å) if the manganous ion were located in the plane of the ring ~2.1 Å away from N-7. The distances are too short to be compatible with an interaction of the manganous ion with N-7 through an intermediate water molecule and are also incompatible with close association of the manganous ion with O-6, in which case the Mn–H-8 distance would be expected to be considerably greater than observed.

The observed average distances from the manganous ion to the purine carbon atoms C-2 and C-4 allow discrimination among the four extreme purine dimer structures shown in Figure 5. The average distances from the manganous ion to C-2 and C-4 were found to be nearly equal and longer than those from the manganous ion to C-5, C-6, and C-8. For both of the head-to-head dimers (Figure 5A and C), distances from the manganous ion to the individual C-2 atoms should be considerably longer than those to C-4. The head-to-tail dimer shown in Figure 5D would be expected to show short manganous ion contacts of ~3.3 Å to C-2 and C-4 of the adjacent ring. In the head-to-tail dimer shown in Figure 5B with both carbonyls on the same edge of the stack, the distance from the manganous ion to C-4 of either purine ring is about the same as that to C-2 on one of the rings, but the distance from the manganous ion to the other C-2 is much greater. Because of the heavy weighting of short contacts in the measured paramagnetic relaxation rate arising from the r^{-6} dependence of T_{1p}, the average Mn–C distances to both C-2 and C-4 as seen by the effect on the relaxation rates would be similar. Thus, a structure similar to that shown for dimer 5B seems to be preferred. It is interesting that neither arrangement 5C nor 5D will allow further association involving H bonding, for example, octamer formation.

The increase in the average manganous ion–H-8 distance resulting from the second equilibrium at high nucleotide concentration requires exclusion of manganous ion from the N-7 interaction site. The formation of a molecular aggregate such as the octamer shown in Figure 6, in which dimers or stacks are held together by two asymmetric hydrogen bonds between N-7 and NH_2(C-2) and between O-6 and NH-1, would cause an increase in the average Mn–H-8 distance by excluding N-7 but not the phosphates from metal coordination, and we propose these ordered molecular aggregates as the probable contributors to the solution structures of GDP and GTP at higher concentrations.

Association of guanosine nucleotides through hydrogen bonding is a well-established phenomenon. Thus, several models for aggregation of the sodium salt of 5′-GMP proposed in the literature incorporate the concept of hydrogen-bonded structures utilizing N-7, including those based upon a stacked tetrameric GMP arrangement,[3-9] helical GMP aggregates,[26] and stacked asymmetric hydrogen-bonded dimers.[27] In the tetramer model four guanosine nucleotides are internally hydrogen bonded in a closed tetramer loop, which further stacks in solution to form octameric units. For the helical model the tetrameric ring is not closed, but rather forms the first turn of a helical chain of hydrogen-bonded nucleotides. In the asymmetric stacked dimer model, the stacked dimers are held together by hydrogen bonds to N-7, but without closing the loop. This model has been questioned on the basis of the observed stoichiometry of nucleotide aggregations and the relative integrated intensities of proton resonances.[7,8]

In a broader sense, the existence of octameric units in solutions of guanosine nucleotides might be expected based on the interpretation of X-ray fiber diffraction data[28] of poly(rG) in terms of a four-strand helix. Furthermore, this four-stranded form of poly(rG) can be destabilized by substitution of the tetraethylammonium cation for the sodium ion, thereby leading to monomeric chains.[29]

Although GDP and GTP intermolecular interactions may be somewhat different from those of GMP due to the higher charge on the phosphate chains, the data indicate that the ordering of the structure in solution is similar to that observed with the sodium

(23) Levy, G. C.; Dechter, J. J. *J. Am. Chem. Soc.* **1980**, *102*, 6191–6196.
(24) DeMeester, P.; Goodgame, D. M. L.; Jones, T. J.; Skapski, A. C. *Biochem. J.* **1974**, *139*, 791–792.
(25) DeMeester, P.; Goodgame, D. M. L.; Skapski, A. C.; Smith, B. T. *Biochim. Biophys. Acta* **1974**, *340*, 113–115.
(26) Sasisekharan, V.; Zimmerman, S.; Davies, D. R. *J. Mol. Biol.* **1975**, *92*, 171–179.
(27) Petersen, S. B.; Led, J. J.; Johnston, E. R.; Grant, D. M. *J. Am. Chem. Soc.* **1982**, *104*, 5007–5015.
(28) Zimmerman, S. B.; Cohen, G. H.; Davies, D. R. *J. Mol. Biol.* **1975**, *92*, 181–192.
(29) Howard, F. B.; Frazier, J.; Miles, H. T. *Biopolymers* **1977**, *16*, 791–809.

salt of 5'-GMP. The data available for ordered association of the sodium salt of 5'-GMP most strongly support the octamer model, and this structure appears most consistent with the data for GDP and GTP. In particular, the existence of two equilibria for GDP and GTP is inconsistent with the helical association model, which would be envisioned as involving stepwise additions of nucleotide units held together by hydrogen bonding. The data indicating initial formation of stacked nucleotide dimers at low concentrations followed by a hydrogen-bonding association of dimers at concentrations greater than 190 mM are also consistent with the observation that highly ordered octameric units of GMP are not detected until nucleotide concentrations of 190 mM are reached[7] and, furthermore, explain the inability of others to observe tetrameric units.

In summary, base stacking of guanosine nucleotides is the primary self-associative process of low-concentration solutions (<100 mM) occurring at 25 °C. This association appears to be insensitive to the number of phosphate groups. A stacking pattern consistent with the data has the purine rings lying head to tail with the N-9 atoms on the same edge of the stack. The phosphate chain is the primary site of interaction of the guanosine nucleotides with manganous ion, and N-7 is the likely secondary site of association. At nucleotide concentrations greater than 190 mM we propose that stacked guanosine nucleotides associate by the formation of asymmetric hydrogen bonds to form octameric units.

Acknowledgment. We thank the National Institutes of Health (GM 25668-01) for support of this work and the Dreyfus Foundation for support of the purchase of the JEOL spectrometer used for many of the studies.

Registry No. GDP, 146-91-8; GTP, 86-01-1; manganous ion, 16397-91-4.

X-ray Structure Analyses and Vibrational Spectral Measurements of the Model Compounds of the Liquid-Crystalline Arylate Polymers. Finding Out the Raman Bands Characteristic of the Twisted Biphenyl Structure in Association with the Solid-to-Liquid Crystalline Phase Transition

Kohji Tashiro,*,† Jian-an Hou,† Masamichi Kobayashi,† and Toshihide Inoue‡

Contribution from the Department of Macromolecular Science, Faculty of Science, Osaka University, Toyonaka, Osaka 560, Japan, and The Research Association of Polymer Basic Technology, Toranomon, Kanda, Tokyo 101, Japan. *Received January 11, 1990*

Abstract: X-ray structural analyses and Raman spectral measurements have been made for two crystal modifications of the model compound of the liquid-crystalline arylate polymers: $EtOCOPhOCO(Ph)_2COOPhCOOEt$. The crystal data determined at room temperature for the α and β forms are as follows: α, monoclinic, $Pn\text{-}C^2_s$, a = 32.620 (5) Å, b = 5.847 (1) Å, c = 14.115 (2) Å, β = 98.19 (1)°, Z = 4, R = 0.057; β, monoclinic, $P2_1/c\text{-}C^5_{2h}$, a = 29.491 (4) Å, b = 5.4405 (3) Å, c = 8.3375 (8) Å, β = 94.890 (8)°, Z = 2, R = 0.072. The main difference in the molecular conformation between these two crystalline forms is a torsional angle between the two benzene rings of the biphenyl group: 48° for the α form and 0° for the β form. This conformational difference correlates to the difference in the characteristic Raman spectral pattern. For example, the 420- and 320-cm^{-1} Raman bands are observed only for the α form and can be utilized as a useful index for the twisted structure of the biphenyl group. The α form was found to transform into the β form at ca. 110 °C and then into the liquid-crystalline state (LC) at ca. 185 °C. The 420- and 320-cm^{-1} Raman bands disappeared in the α-to-β transition and reappeared in the β-to-LC transition, suggesting that the biphenyl group takes a twisted structure in the liquid-crystalline state as well as in the α crystal.

Recently a large amount of attention has been paid to the liquid-crystalline arylate polymers such as poly-*p*-oxybenzoyl, its copolymers with polyethylene terephthalate, etc., because of their excellent mechanical properties of high Young's modulus, high strength, and good processability.[1] These polymers experience a crystal-to-liquid crystal-phase transition at high temperature.[2] Spinning from the liquid-crystalline phase is one of the important processes to produce the mechanically strong fiber. Then it is required to clarify what type of structural change may occur during this phase transition. In general, however, the liquid-crystalline polymers show the very poor X-ray fiber patterns with quite a small number of broad reflections, making it practically impossible to perform the detailed structural analyses. In such a situation, a utilization of the model compounds may provide us with a chance to obtain a variety of useful information concerning the structural changes occurring in the phase transition of the liquid-crystalline polymers.

We have been studying a relationship between the crystal structure and the vibrational spectra of the following series of the model compounds so as to find out some important and useful indices necessary for clarifying the structure of the liquid-crystalline state. In the present study, the compound with n = 2 has

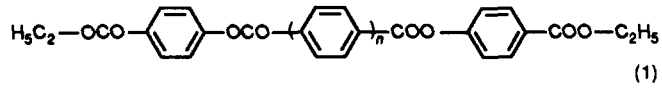

(1)

been selected which serves as a model for the liquid-crystalline

† Osaka University.
‡ The Research Association of Polymer Basic Technology.

(1) Chung, T. *Polym. Eng. Sci.* **1986**, *26*, 901.
(2) Varshney, S. K. *J. Macromol. Sci.—Rev. Macromol. Chem. Phys.* **1986**, *C26*, 551.

0002-7863/90/1512-8273$02.50/0